Proceedings of the ASME 2014 International Design Engineering Technical Conferences & Computers and Information in Engineering Conference
IDETC/CIE 2014
August 17-20, 2014, Buffalo, New York, USA

DETC2014-35203

A UNIFIED ALGORITHM FOR ANALYSIS AND SIMULATION OF PLANAR FOUR-BAR MOTIONS DEFINED WITH R- AND P-JOINTS

Xiangyun Li, Xin Ge, Anurag Purwar, Q.J.Ge*

Computational Design Kinematics Lab
State University of New York at Stony Brook
Stony Brook, New York, 11794-2300

ABSTRACT

This paper presents a single, unified and efficient algorithm for animating the motions of the coupler of all four-bar mechanisms formed with revolute (R) and prismatic (P) joints. This is achieved without having to formulate and solve the loop closure equation associated with each type of four-bar linkages separately. In our previous paper on four-bar linkage synthesis, we map the planar displacements from Cartesian to image space using planar quaternion. Given a set of image points that represent planar displacements, the problem of synthesizing a planar four-bar linkage is reduced to finding a pencil of Generalized- or G-manifolds that best fit the image points in the least squares sense. The three planar dyads associated with Generalized G-manifolds are RR, PR and RP which could construct six types of four-bar mechanisms. In this paper, we show that the same unified formulation for linkage synthesis leads to a unified algorithm for linkage analysis and simulation as well. Both the unified synthesis and analysis algorithms have been implemented on Apple's iOS platform.

1 Introduction

This paper revisits the well-studied problem of kinematic analysis of planar four-bar linkages formed with revolute (R) and prismatic (P) joints. The solutions to this problem are well known and are available in undergraduate textbooks on mechanism design and analysis. Typically, the problem is solved using the so-called vector loop closure equation which is formulated for a specific type of planar four-bar linkages such as planar RRRR or RRRP (slider-crank) mechanism. Recently, we have developed a unified algorithm for simultaneous type and dimensional synthesis of planar four-bar linkages [1]. With the unified algorithm, we are able to determine the type of joints, either R or P, as well as the dimensions, simultaneously for finite position synthesis. In this paper, we seek to develop a unified algorithm for analysis and simulation of the resulting four-bar linkage, without having to know the mechanism type and then formulate the loop closure equation specifically for that particular type of mechanism. This has the potential to greatly improve efficiency of the software development and maintenance.

There have been significant academic and commercial research efforts in the development of software systems for the synthesis and animation of planar four-bar mechanisms such as SyMech [2], WATT [3], SAM [4] and Adams [5]. They provide facilities to synthesize and animate the planar 4R linkage whose four joints are all revolute joints. In order to animate the coupler motion of planar 4R linkage, loop-closure equation method (see Norton [6]) is used to find the coupler angle when the input link rotates. In our previous paper [1], we presented a task driven approach to simultaneous type and dimensional synthesis of planar four-bar linkages using algebraic fitting of a pencil of G-manifolds. In general, there are at most six possible types of four-bar mechanisms that can be constructed, which are RRRR, RRRP, RRPR, PRPR, PRRP and RPPR. The advantage of our approach is that given a prescribed task motion, it can determine

*Address all correspondence to this author: Qiaode.Ge@stonybrook.edu.

all the possible four-bar types together with their dimensions for motion generation. We have recently implemented our unified synthesis algorithm on iOS platform. Fig. 1 shows the screen shot of the graphical user interface (GUI) of the design program on iPad. In terms of the animation part, we have only implemented planar RRRR linkage which uses the traditional method of loop-closure equation. We plan to include the animation codes for other four-bar linkage types as well. However, if the method of loop-closure equation continues to be used, we have to write six different versions of animation code for each four-bar type, leading to code redundancy and maintenance problem. Thus, it makes sense to have a unified algorithm for animating all six types of four-bar mechanisms.

We use a planar quaternion formulation to transform the task positions into points in the image space (see Bottema and Roth [7], McCarthy [8], Ravani and Roth [9]). In this way, geometric constraints associated with planar dyads, such as circle or line constraints, are transformed into special quadric surfaces called constraint manifolds. In the process, we discovered a unified equation for the constraint manifolds for all planar dyads, namely, RR, PR, RP and PP. For RR-, PR- and RP-dyad, the quadrics are hyperboloid of one sheet, hyperbolic paraboloid I (HP I) and hyperbolic paraboloid II (HP II), respectively. HP I and II are just regular hyperbolic paraboloids only with the difference of being opening up along negative or positive X-axis. The unified equation defines the generalized manifold, called G-manifold, for all planar dyads. In this way, a planar four-bar motion, when mapped into the image space, becomes the curve of intersection of two G-manifolds. If one can develop a general algorithm for computing the intersection of two G-manifolds, without having to know specifically the type of quadrics before hand, then this algorithm could be used to unify the analysis and simulation of all types of planar four-bar linkages. This, in turn, has the advantage of reducing the cost of software maintenance.

Computing the intersection of two general quadrics is a classical problem in analytic geometry of three dimensions. This problem has been solved from the computer graphics perspective by Levin [10], [11]. It is based on an analysis of the pencil generated by the two quadrics, i.e., the set of linear combinations of the two quadrics. Building on Levin's work, Dupont et al. [12] presented the first practical and efficient algorithm for computing an exact parametric representation of the intersection of two quadric surfaces in three-dimensional space given by implicit equations with rational coefficients. Building on the works by Levin and Dupont et al., we provide a compact and efficient algorithm to find the parametric form for the intersection of two quadrics which are G-manifolds of planar dyads that unifies the representation for hyperboloid of one sheet and hyperbolic paraboloid.

The organization of the paper is as follows. Section 2 reviews the conventional method for analyzing the coupler motion of a planar four-bar linkage. Section 3 presents the advocated algorithm for unifying the computation of the coupler motions generated by various four-bar linkages. Finally, we present six examples for each type of four-bar mechanism to demonstrate the efficacy of our approach.

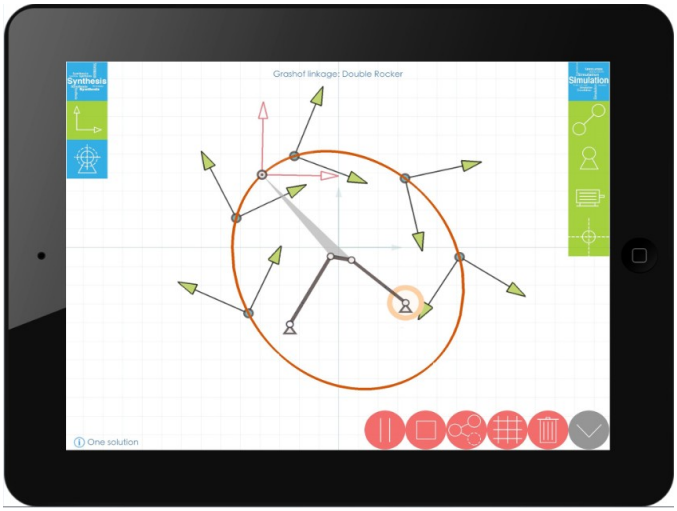

FIGURE 1. The screen shot of graphical user interface on iPad

2 Four-Bar Motion Analysis Based on the Loop-closure Equation

In this section, we review the conventional approach to four-bar motion analysis using loop-closure equation. For simplicity, we use the RRRR-type as an example to outline the procedure.

Consider a planar 4R linkage shown in Fig. 2 with XOY being the fixed coordinate frame. The fixed pivot A_0 is located at point (x_0, y_0) with A_0B_0 being the ground link and A_0A the input link. Let l_i denote the length of the ith link and θ_1 the angle measured from the X axis of the fixed frame. Let ϕ, λ and ψ be the angles of link A_0A, AB, B_0B as measured from the ground link A_0B_0, respectively. A moving frame is attached to coupler link AB at P with β measured from AB to to its x-axis. Polar coordinates (r, α) represent the position of P with respect to coupler AB. All the quantities except λ and ψ are known values after synthesis. When animating the 4R linkage, we rotate the input link A_0A with ϕ being known at a given moment. In order to calculate the position and orientation of moving frame relative to XOY at each value of ϕ, the key is to find the coupler angle λ.

Using loop-closure equation (Norton [6] and Wu et al. [13]), the relationship between coupler angle λ and input link angle ϕ is given by

$$e^{i\lambda} = \frac{-B(\phi) \pm \sqrt{\Delta_1(\phi)\Delta_2(\phi)}}{2A(\phi)} \tag{1}$$

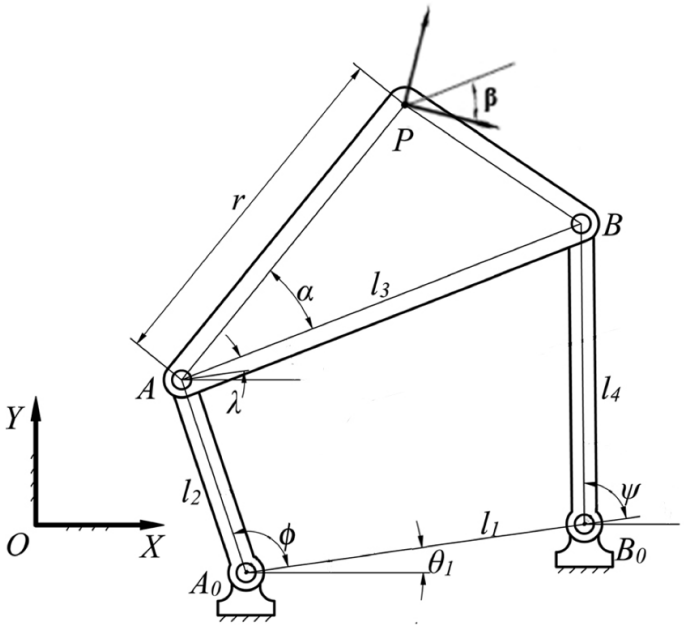

FIGURE 2. A planar 4R mechanism

where

$$A(\phi) = l_{31}(l_{21}e^{-j\phi} - 1) \tag{2}$$
$$B(\phi) = 1 + l_{21}^2 + l_{31}^2 - l_{41}^2 - 2l_{21}\cos\phi \tag{3}$$
$$\Delta_1(\phi) = 1 + l_{21}^2 - (l_{31} + l_{41})^2 - 2l_{21}\cos\phi \tag{4}$$
$$\Delta_2(\phi) = 1 + l_{21}^2 - (l_{31} - l_{41})^2 - 2l_{21}\cos\phi \tag{5}$$
$$l_{21} = l_2/l_1,\ \ l_{31} = l_3/l_1,\ \ l_{41} = l_4/l_1 \tag{6}$$

and the sign $\pm$ correspond to the two configurations of the four-bar linkage for the same input angle.

With λ being known, the position of moving frame, i.e., the position vector **P** of its origin P can be obtained by the following vector addition

$$\mathbf{OP} = \mathbf{OA}_0 + \mathbf{A}_0\mathbf{A} + \mathbf{AP} \tag{7}$$

where

$$\mathbf{OA}_0 = [x_0, y_0] \tag{8}$$
$$\mathbf{A}_0\mathbf{A} = [l_2\cos(\phi + \theta_1), l_2\sin(\phi + \theta_1)] \tag{9}$$
$$\mathbf{AP} = [r\cos(\alpha + \lambda + \theta_1), r\sin(\alpha + \lambda + \theta_1)] \tag{10}$$

The orientation of moving frame is calculated as

$$orientation = \theta_1 + \lambda + \beta \tag{11}$$

Moreover, the position of moving pivot A and B can be easily obtained as follows

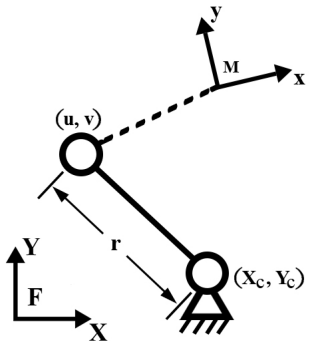

FIGURE 3. RR Dyad

$$\mathbf{OA} = \mathbf{OA}_0 + \mathbf{A}_0\mathbf{A} \tag{12}$$
$$\mathbf{OB} = \mathbf{OA}_0 + \mathbf{A}_0\mathbf{A} + \mathbf{AB} \tag{13}$$

where

$$\mathbf{AB} = [l_3\cos(\lambda + \theta_1), l_3\sin(\lambda + \theta_1)] \tag{14}$$

With the computed position and orientation of moving frame and coordinates of moving pivots , we are now able to draw the planar 4R mechanism with its coupler motion at each frame of animation. However, this loop-closure equation is only valid for planar RRRR linkage. A different type of planar four-bar linkages calls for a different loop closure equation. This means that one has to write six separate codes for all six types of planar four-bar linkages. In next section, our approach will be presented which has the benefit of unifying the kinematic analysis codes.

3 A Unifed Algorithm for General Four-Bar Motion Analysis

In [1] we presented a unified equation for the constraint manifolds of all types of planar dyads formed with R and P joints. This transforms the problem of general four-bar motion analysis into that of computing the intersection of two G-manifolds in image space. The latter problem can be readily solved by applying methods developed in the context of computer graphics.

3.1 Dyads and G-manifolds

Consider three types of dyads, RR, PR and RP. Their kinematic diagram are shown in Figure 3, 4 and 5.

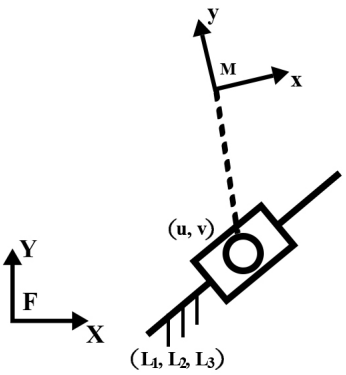

FIGURE 4. PR Dyad

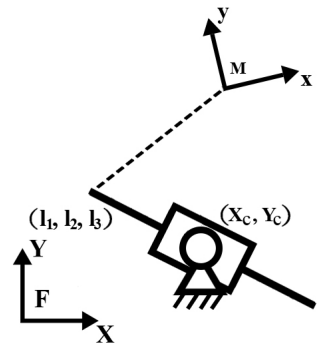

FIGURE 5. RP Dyad

The design parameters of a RR dyad are fixed pivot coordinates (X_c, Y_c) relative to the fixed frame **F**, moving pivot coordinates (u, v) relative to the moving frame **M** and the length r of the first link. The design parameters of PR dyad are sliding axis coordinates (L_1, L_2, L_3) of P joint relative to **F** and the moving pivot coordinates (u, v) relative to **M**. The design parameters of RP dyad are fixed pivot coordinates (X_c, Y_c) relative to **F** and sliding axis coordinates (l_1, l_2, l_3) of P joint relative to **M**.

Let (d_1, d_2) denote the coordinates of the origin of **M** with respect to **F**, and α denote the rotation angle of **M** relative to **F**. Planar quaternion introduces the following mapping from Cartesian space parameters (d_1, d_2, α) to image space coordinates $\mathbf{Z} = (Z_1, Z_2, Z_3, Z_4)$ (see [7]):

$$\begin{aligned} Z_1 &= (d_1/2)\sin(\alpha/2) - (d_2/2)\cos(\alpha/2) \\ Z_2 &= (d_1/2)\cos(\alpha/2) + (d_2/2)\sin(\alpha/2) \\ Z_3 &= \sin(\alpha/2) \\ Z_4 &= \cos(\alpha/2) \end{aligned} \tag{15}$$

where (Z_1, Z_2, Z_3, Z_4) are homogeneous coordinates of the image space, which is a projective three-space $\mathbb{P}^3(\mathbb{R})$. The inverse relationship from an image point to coordinates in the Cartesian space is

$$\begin{aligned} d_1 &= 2(Z_1Z_3 + Z_2Z_4)/(Z_3^2 + Z_4^2) \\ d_2 &= 2(Z_2Z_3 - Z_1Z_4)/(Z_3^2 + Z_4^2) \\ \cos\alpha &= (Z_4^2 - Z_3^2)/(Z_3^2 + Z_4^2) \\ \sin\alpha &= 2Z_3Z_4/(Z_3^2 + Z_4^2) \end{aligned} \tag{16}$$

The two DOF motions of RR-, PR- and RP-dyads, are represented by surfaces called G-manifolds in image space. Based on [1], the homogeneous algebraic equation of G-manifold is given by

$$\begin{aligned} &q_1(Z_1^2 + Z_2^2) + q_2(Z_1Z_3 - Z_2Z_4) + q_3(Z_2Z_3 + Z_1Z_4) \\ &+q_4(Z_1Z_3 + Z_2Z_4) + q_5(Z_2Z_3 - Z_1Z_4) + q_6Z_3Z_4 \\ &+q_7(Z_3^2 - Z_4^2) + q_8(Z_3^2 + Z_4^2) = 0 \end{aligned} \tag{17}$$

with the coefficients q_i satisfying the following two relations:

$$\begin{aligned} q_1q_6 + q_2q_5 - q_3q_4 &= 0 \\ 2q_1q_7 - q_2q_4 - q_3q_5 &= 0. \end{aligned} \tag{18}$$

Eq.(17) represents in general a hyperboloid of one sheet for a RR dyad. It represents a hyperbolic paraboloid I for a PR dyad when $q_1 = q_2 = q_3 = 0$ and a hyperbolic paraboloid II for a RP dyad when $q_1 = q_4 = q_5 = 0$.

Eq.(17) can be rewritten in matrix form as $Q_G = \mathbf{Z}^T[G]\mathbf{Z} = 0\}$ where

$$[G] = \begin{bmatrix} q_1 & 0 & \frac{q_2+q_4}{2} & \frac{q_3-q_5}{2} \\ 0 & q_1 & \frac{q_3+q_5}{2} & \frac{q_4-q_2}{2} \\ \frac{q_2+q_4}{2} & \frac{q_3+q_5}{2} & q_7+q_8 & \frac{q_6}{2} \\ \frac{q_3-q_5}{2} & \frac{q_4-q_2}{2} & \frac{q_6}{2} & q_8-q_7 \end{bmatrix}. \tag{19}$$

Once a linkage has been synthesized, one can obtain the values of q_i from the original design parameters of its associated dyad (see [1]). With the intersection algorithm to be presented later on, the parameterization $\mathbf{Z}(t)$ for the intersection curve can be determined, and then the position and orientation of **M** can be obtained through Eq. (16). With the **M** being calculated at each time instant, those dyad design parameters relative to **M**, i.e., moving joints or moving lines, can be determined relative to **F**. Upon working out all the instantaneous information about **M** and moving joint or lines, the four-bar motion can then be animated.

3.2 The Intersection Algorithm

Given two G-manifolds Q_{G_1} and Q_{G_2}, the outline of intersection algorithm is as follows (Dupont et al. [12]):

1. Construct the orthonormal transformation matrix $[P]$ which converts G_1 into diagonal matrix $\tilde{G}_1$ by computing the eigenvalues and the normalized eigenvectors of G_1. The same matrix $[P]$ sends Q_{G_1} into canonical form $Q_{\tilde{G}_1}$. Determine the parameterization $\mathbf{Z}(u,v) = [Z_1(u,v), Z_2(u,v), Z_3(u,v), Z_4(u,v)]$ of the canonical quadric $Q_{\tilde{G}_1}$.
2. Compute the matrix $[\tilde{G}_2] = [P]^T[G_2][P]$ for the quadric Q_{G_2} which transforms Q_{G_2} into $Q_{\tilde{G}_2}$. Substitute $\mathbf{Z}(u,v)$ into the algebraic equation of $Q_{\tilde{G}_2}$, i.e., $\mathbf{Z}^T[\tilde{G}_2]\mathbf{Z} = 0$, to obtain the following equation

$$\mathbf{Z}(u,v)^T[\tilde{G}_2]\mathbf{Z}(u,v) = a(v)u^2 + b(v)u + c(v) = 0. \quad (20)$$

   Then solve Eq. (20) for u in terms of v and use $\Delta(v) = b^2(v) - 4a(v)c(v) \geq 0$ to determine the domain of v such that real solutions exist for u and we denote the real solutions as $u(v)$. Substitute $u(v)$ into $\mathbf{Z}(u,v)$ to get the parameterization $\mathbf{Z}(v)$ for the intersection of $Q_{\tilde{G}_1}$ and $Q_{\tilde{G}_2}$.
3. Finally, $[P]\mathbf{Z}(v)$ is the parameterization for the intersection of Q_{G_1} and Q_{G_2}.

During Step 1, the canonical form $Q_{\tilde{G}_1}$ stays the same as

$$aZ_1^2 + bZ_2^2 - cZ_3^2 - dZ_4^2 = 0 \quad (21)$$

regardless whether Q_{G_1} is a hyperboloid of one sheet or hyperbolic paraboloid I or hyperbolic paraboloid II. The parameterization $\mathbf{Z}(u,v)$ is given as (Dupont et al. [12]):

$$\mathbf{Z}(u,v) = [\frac{u+av}{a}, \frac{uv-b}{b}, \frac{u-av}{\sqrt{ac}}, \frac{uv+b}{\sqrt{bd}}] \quad (22)$$

In Step 3, $a(v)$, $b(v)$ and $c(v)$ are polynomials of degree at most two in v due to the bilinearity of $\mathbf{Z}(u,v)$. Therefore, $\Delta(v)$ is a polynomial of degree up to four.

Over the course of the algorithm, there is no need to distinguish among the three types of G-manifolds associated with planar RR, PR and RP dyads, and thereby unifies the coupler motion generation code.

4 Examples and Discussions

Now, we present six examples for the planar RRRR, RRRP, RRPR, PRPR, PRRP and RPPR linkages. For each example, the inputs are two G-manifolds corresponding to two dyads that make up a specific four-bar linkage. The two G-manifolds are represented by their algebraic equations Eq. (17). The outputs are intersection curves of the two G-manifolds. Since the G-manifolds are represented using homogeneous equation (Z_1, Z_2, Z_3, Z_4), for visualization purpose, we project the G-manifold onto the the hyperplane $Z_4 = 1$.

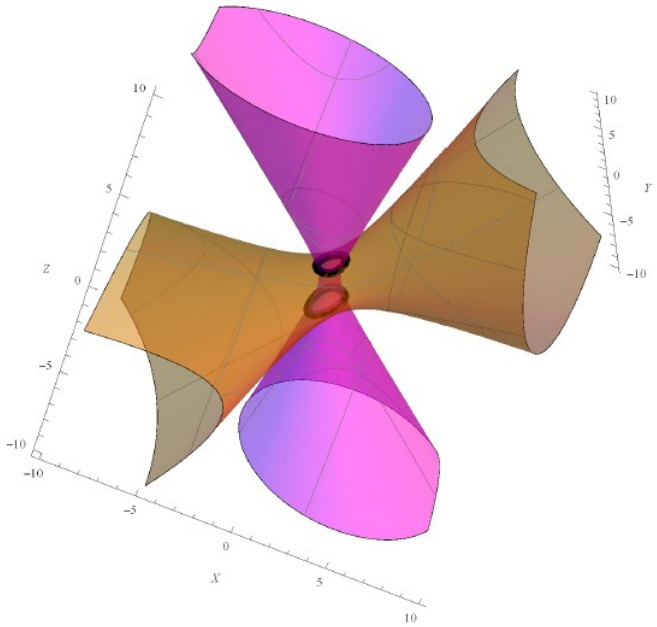

FIGURE 6. Two G-manifolds (hyperboloids of one sheet) and their intersection curve.

4.1 Example: Planar RRRR Linkage

Consider a planar RRRR linkage whose G-manifolds associated with two RR dyads are given by

$$\begin{aligned} RR1: \; & -2(Z_1^2+Z_2^2)+9.18(Z_1Z_3-Z_2Z_4)+2.68(Z_2Z_3+Z_1Z_4) \\ & +2.3(Z_1Z_3+Z_2Z_4)+0.76(Z_2Z_3-Z_1Z_4)+0.4064Z_3Z_4 \\ & -5.7877(Z_3^2-Z_4^2)-1.252(Z_3^2+Z_4^2)=0 \quad (23) \\ RR2: \; & -2(Z_1^2+Z_2^2)+2.48(Z_1Z_3-Z_2Z_4)+0.2(Z_2Z_3+Z_1Z_4) \\ & -4.4(Z_1Z_3+Z_2Z_4)-0.2(Z_2Z_3-Z_1Z_4)+0.192Z_3Z_4 \\ & +2.738(Z_3^2-Z_4^2)-2.43265(Z_3^2+Z_4^2)=0 \quad (24) \end{aligned}$$

The two G-manifolds and their intersection are shown in Fig. 6. In this case, both G-manifolds happen to be hyperboloids of one sheet and their curve of intersection has two branches. Each branch corresponds to one configuration of the planar four-bar mechanism.

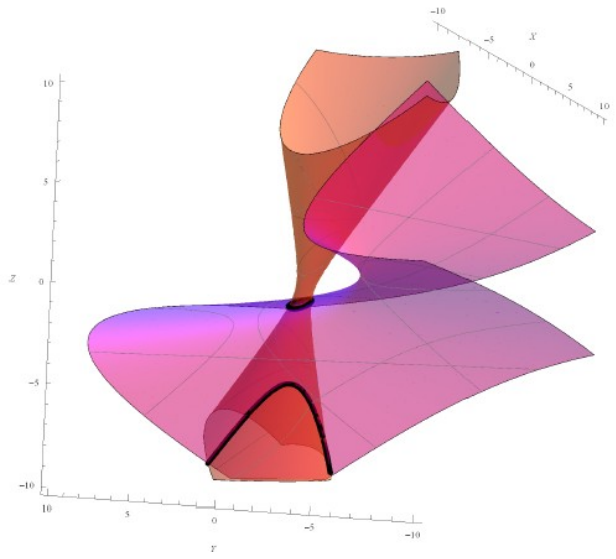

FIGURE 7. The G-manifolds of a crank-slider mechanism.

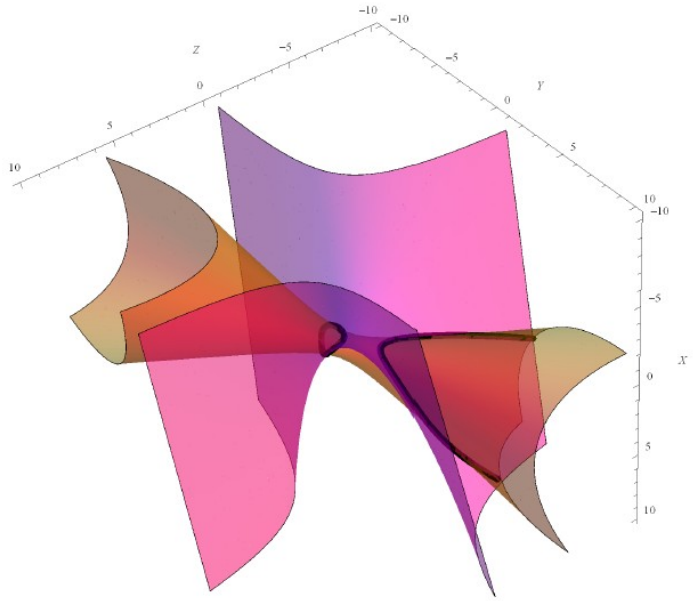

FIGURE 8. The G-manifolds of a swing-block mechanism.

4.2 Example: RRRP

Consider an example for RRRP (Crank-Slider) mechanism. The two algebraic equations of constraint manifolds corresponding to RR and PR are

$$\begin{aligned} RR: & -2(Z_1^2+Z_2^2)-4(Z_1Z_3-Z_2Z_4)-6(Z_2Z_3+Z_1Z_4) \\ & +0(Z_1Z_3+Z_2Z_4)+2(Z_2Z_3-Z_1Z_4)-4Z_3Z_4 \\ & +3(Z_3^2-Z_4^2)-6.5(Z_3^2+Z_4^2)=0 \qquad (25) \\ PR: & \ 0(Z_1^2+Z_2^2)+0(Z_1Z_3-Z_2Z_4)+0(Z_2Z_3+Z_1Z_4) \\ & +2(Z_1Z_3+Z_2Z_4)+4(Z_2Z_3-Z_1Z_4)+10Z_3Z_4 \\ & +5(Z_3^2-Z_4^2)+1(Z_3^2+Z_4^2)=0 \qquad (26) \end{aligned}$$

The G-manifolds and their intersection curve are shown in Fig. 7. One G-manifold is hyperboloid of one sheet and the other one hyperbolic paraboloid I. In this case, the curve of intersection has also two branches and each corresponds to one configuration of Crank-Slider mechanism.

4.3 Example: RRPR

Consider an example for RRPR (Swing-Block) mechanism. The two algebraic equations of constraint manifolds corresponding to RR and RP are

$$\begin{aligned} RR: & -2(Z_1^2+Z_2^2)-4(Z_1Z_3-Z_2Z_4)-5.98(Z_2Z_3+Z_1Z_4) \\ & +0(Z_1Z_3+Z_2Z_4)+2(Z_2Z_3-Z_1Z_4)-4Z_3Z_4 \\ & +2.99(Z_3^2-Z_4^2)-4.9711(Z_3^2+Z_4^2)=0 \qquad (27) \end{aligned}$$

$$\begin{aligned} RP: & \ 0(Z_1^2+Z_2^2)+0(Z_1Z_3-Z_2Z_4)+2(Z_2Z_3+Z_1Z_4) \\ & +0(Z_1Z_3+Z_2Z_4)+0(Z_2Z_3-Z_1Z_4)-4Z_3Z_4 \\ & -3(Z_3^2-Z_4^2)+3(Z_3^2+Z_4^2)=0 \qquad (28) \end{aligned}$$

The intersection curves are shown in Fig. 8. One G-manifold is hyperboloid of one sheet and the other one hyperbolic paraboloid II. There are two branches of the intersection curve and each corresponds to one configuration of Swing-Block mechanism.

4.4 Example: PRPR

Consider an example for PRPR (Slider-Swinging Block) mechanism. The two algebraic equations of constraint manifolds corresponding to PR and RP are

$$\begin{aligned} PR: & \ 0(Z_1^2+Z_2^2)+0(Z_1Z_3-Z_2Z_4)+0(Z_2Z_3+Z_1Z_4) \\ & +2(Z_1Z_3+Z_2Z_4)+2(Z_2Z_3-Z_1Z_4)-16Z_3Z_4 \\ & +4.0034(Z_3^2-Z_4^2)+2.0017(Z_3^2+Z_4^2)=0 \qquad (29) \\ RP: & \ 0(Z_1^2+Z_2^2)+0(Z_1Z_3-Z_2Z_4)+2(Z_2Z_3+Z_1Z_4) \\ & +0(Z_1Z_3+Z_2Z_4)+0(Z_2Z_3-Z_1Z_4)-5.9994Z_3Z_4 \\ & +2(Z_3^2-Z_4^2)-2(Z_3^2+Z_4^2)=0 \qquad (30) \end{aligned}$$

The intersection curves are shown in Fig. 9. One G-manifold is hyperbolic paraboloid I and the other one hyperbolic paraboloid II. There are two branches for the intersection curve and each corresponds to one configuration of Slider-Swinging Block mechanism.

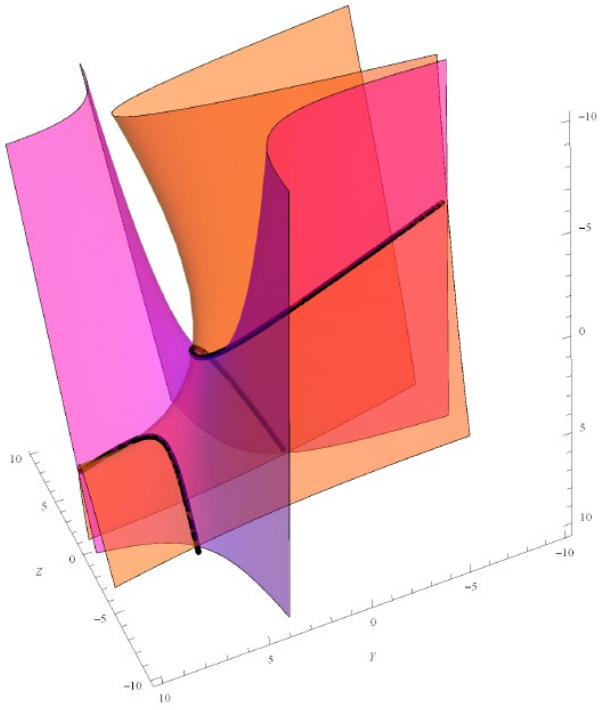

FIGURE 9. The G-manifolds of a slider-swinging block mechanism.

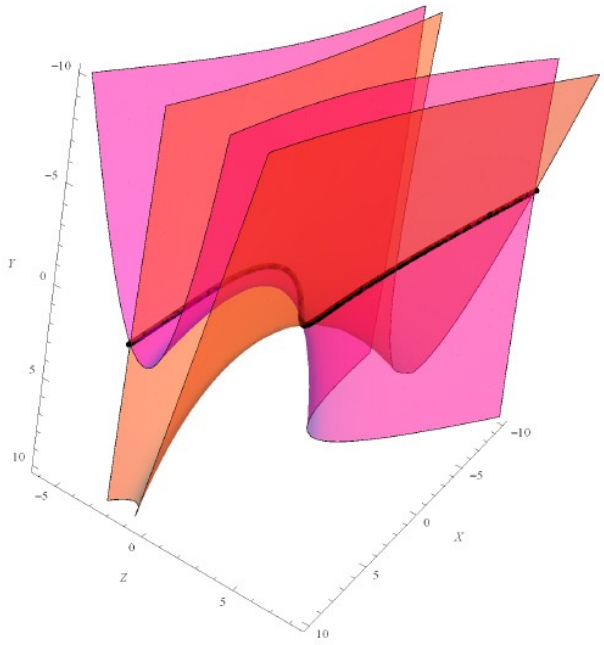

FIGURE 10. The G-manifolds of the double-slider mechanism.

4.5 Example: PRRP

Consider an example for PRRP (Double-Slider) mechanism. The two algebraic equations of constraint manifolds corresponding to the two PR dyads are

$$\begin{aligned} PR1: \quad & 0(Z_1^2+Z_2^2)+0(Z_1Z_3-Z_2Z_4)+0(Z_2Z_3+Z_1Z_4) \\ & +1.8632(Z_1Z_3+Z_2Z_4)-0.727(Z_2Z_3-Z_1Z_4)-5.8423Z_3Z_4 \\ & +3.0797(Z_3^2-Z_4^2)+0.5684(Z_3^2+Z_4^2)=0 \qquad (31) \\ PR2: \quad & 0(Z_1^2+Z_2^2)+0(Z_1Z_3-Z_2Z_4)+0(Z_2Z_3+Z_1Z_4) \\ & +1.8566(Z_1Z_3+Z_2Z_4)+0.7438(Z_2Z_3-Z_1Z_4)-10.9583Z_3Z_4 \\ & +3.4351(Z_3^2-Z_4^2)+1.2995(Z_3^2+Z_4^2)=0 \qquad (32) \end{aligned}$$

The intersection curve is shown in Fig. 10. Both G-manifolds are hyperbolic paraboloid I. There is only one intersection curve corresponding to the single configuration of Double-Slider mechanism.

4.6 Example: RPPR

Consider an example for RPPR (Double-Swinging Block) mechanism. The two algebraic equations of constraint manifolds corresponding to the two RP dyads are

$$\begin{aligned} RP1: \quad & 0(Z_1^2+Z_2^2)+0.4712(Z_1Z_3-Z_2Z_4)+1.9438(Z_2Z_3+Z_1Z_4) \\ & +0(Z_1Z_3+Z_2Z_4)+0(Z_2Z_3-Z_1Z_4)+0.4973Z_3Z_4 \\ & -0.0243(Z_3^2-Z_4^2)+4.0818(Z_3^2+Z_4^2)=0 \qquad (33) \\ RP2: \quad & 0(Z_1^2+Z_2^2)+1.8574(Z_1Z_3-Z_2Z_4)-0.7418(Z_2Z_3+Z_1Z_4) \\ & +06(Z_1Z_3+Z_2Z_4)+0(Z_2Z_3-Z_1Z_4)+3.4594Z_3Z_4 \\ & -3.7661(Z_3^2-Z_4^2)+4.2042(Z_3^2+Z_4^2)=0 \qquad (34) \end{aligned}$$

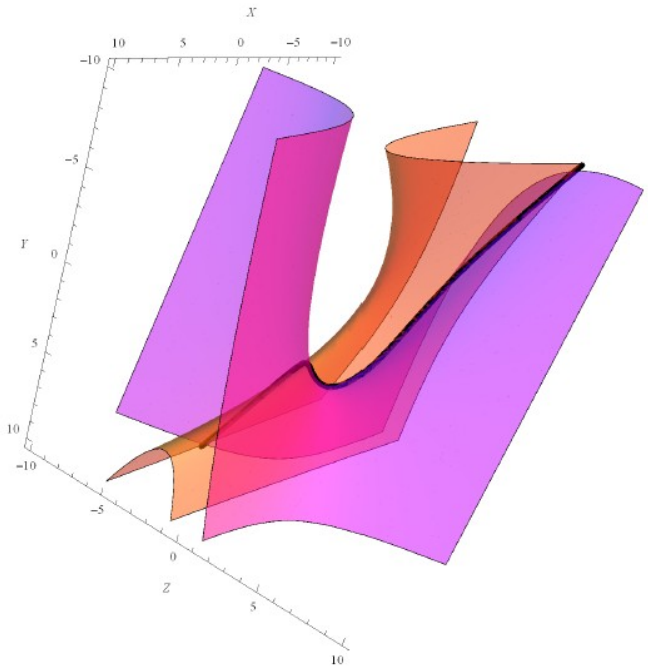

FIGURE 11. The G-manifolds of a double-swinging block mechanism.

The intersection curve is shown in Fig. 11. Both G-manifolds are hyperbolic paraboloid II. The intersection curve has only one branch which corresponds to the single configuration of Double-Swinging Block mechanism.

5 Conclusions

In this paper, we presented a unified algorithm to the analysis and simulation of all types of planar four-bar motions. Instead of taking the approach of loop-closure equation towards simulations of different four-bar types, we employ planar quaternion to map a four-bar mechanism into a pair of G-manifold in image space and therefore the four-bar coupler motion ends up being the intersection curves. The animation problem is then reduced to the problem of determining the parameterization for the intersection curves. Since our G-manifolds are in the category of quadrics, and limited to hyperboloid of one sheet and hyperbolic paraboloid, there exists a simple and efficient algorithm to find the parameterization. The six examples provided fully demonstrate the effectiveness of this algorithm.

6 ACKNOWLEDGMENT

The work has been financially supported by National Science Foundation under Collaborative Research grant to Stony Brook University (Q. J. Ge, grant CMMI-0856594). All findings and results presented in this paper are those of the authors and do not represent those of the funding agencies.

REFERENCES

[1] Ge, Q. J., Zhao, P., Purwar, A., 2013. "A Task Driven Approach to Unified Synthesis of Planar Four-Bar Linkages Using Algebraic Fitting Of A Pencil Of G-Manifolds", ASME 2013 International Design Engineering Technical Conferences & Computers and Information in Engineering Conference, Portland, OR, Paper No. DETC2013-12977

[2] SyMech. http://www.symech.com.

[3] WATT. http://www.heron-technologies.com/watt.

[4] SAM. http://www.artas.nl.

[5] Adams. http://www.mscsoftware.com/product/adams.

[6] Norton, R. L., 2012. *Design of Machinery: An Introduction to the Synthesis and Analysis of Mechanisms and Machines, Fifth Edition*. Mcgraw-Hill, New York.

[7] Bottema, O., and Roth, B., 1979. *Theoretical Kinematics*. North Holland, Amsterdam.

[8] McCarthy, J. M., 1990. *Introduction to Theoretical Kinematic*s. MIT, Cambridge, Mass.

[9] Ravani, B., and Roth, B., 1984. "Mapings of spatial kinematics". *Journal of Mechanisms Transmissions and Automation in Design-Transactions of the ASME*, 106(3), pp. 341–347.

[10] Levin, J., 1976. "A parametric algorithm for drawing pictures of solid objects composed of quadric surfaces". *Communications of the ACM*, 19(10), pp. 555–563.

[11] Levin, J., 1979. "Mathematical models for determining the intersections of quadric surfaces". *Computer Graphics and Image Processing*,11(1), pp. 73–87.

[12] Dupont, L., Lazard, D., Lazard S. and Petitjean, S., 2008."Near-optimal parameterization of the intersection of quadrics: I. The generic algorithm, II. A classification of pencils and III. Parameterizing singular intersections", *Journal of Symbolic Computation*, 43(3), pp. 168–232.

[13] Wu, J., Ge, Q. J., Gao, F., and Guo, W. Z., 2011, "On the Extension of a Fourier Descriptor Based Method for Four-Bar Linkage Synthesis for the Generation of Open Curves". *ASME Journal of Mechanisms and Robotics*, 3(3), pp. 031002